ELECTRONIC SUPPLEMENTARY INFORMATION

Nickel hydroxide ultrathin nanosheets as building blocks for electrochemically active layers

Barbora Schneiderová,[a,b] Jan Demel,[a] Josef Pleštil,[c] Pavel Janda,[d] Jan Bohuslav,[d,e] Dris Ihiawakrim,[f] Ovidiu Ersen,[f] Guillaume Rogez,[f] and Kamil Lang[a]*

[a] *Institute of Inorganic Chemistry of the AS CR, v. v. i., Husinec-Řež 1001, 250 68 Řež, Czech Republic, lang@iic.cas.cz*

[b] *Faculty of Science, Charles University in Prague, Hlavova 2030, 128 43 Praha 2,Czech Republic*

[c] *Institute of Macromolecular Chemistry of the AS CR, v. v. i., Heyrovského nám. 2, 162 06 Praha 6, Czech Republic*

[d] *J. Heyrovský Institute of Physical Chemistry of the AS CR, v. v. i., Dolejškova 3, 182 23 Praha 8, Czech Republic*

[e] *Institute of Chemical Technology, Prague, Technická 5, 166 28 Praha 6, Czech Republic*

[f] *Institut de Physique et Chimie des Matériaux de Strasbourg, UMR CNRS-UdS 7504, 23 rue du Loess, BP 43, 67034 Strasbourg Cedex 2, France*

*Corresponding author: Email address: lang@iic.cas.cz, Tel: +420 26617 2193. Fax: +420 22094 1502.

Contents

Syntheses

Nickel lactate. 6.8 mL (22 mmol) of 60 % solution of sodium lactate was added to 20 mL of 1 M solution of nickel chloride. The mixture was stirred at 60 °C for 1 hour. The green precipitate was filtrated and washed three times with water and twice with acetone. The product was air-dried at room temperature and used directly for the syntheses of LNHs.

Layered nickel hydroxide dodecyl sulphate salt (LNH-DS). 1.45 g (5 mmol) of $Ni(NO_3)_2 \cdot 6H_2O$, 5.77 g (20 mmol) of SDS, and 7.01 g (50 mmol) of HMT were dissolved in a mixture of deionised water (90 mL) and 1-butanol (10 mL) and heated to 90 °C for 2 hours. The green precipitate was filtrated, washed three times with water and acetone, and air-dried. The elemental and thermogravimetric analyses confirmed the chemical composition (Table S1).

Voltammetric experiments

Electrochemical experiments were performed using a computer-controlled potentiostat (Wenking POS2, Bank Electronik, Germany) in a three-electrode arrangement. A low-volume electrochemical cell utilized the basal plane HOPG support for the film layers as a working electrode; a platinum wire and a saturated calomel electrode served as a counter and a reference electrode, respectively. Cyclic voltammetry was performed in aqueous (purified by Milli-Q system Gradient, Millipore, resistivity 18.2 MΩ cm) solution of 1M KOH as electrolyte, deoxygenated by argon.

Table S1 Elemental analyses of the prepared LNHs. The values in parenthesis were calculated using the formula $Ni_2(OH)_3A \cdot mH_2O$.

LNHs	Elemental analysis / %			Water content[a] %, [m]	Mass loss %
	C	H	N		
LNH-DS	26.82 (30.67)	5.74 (6.88)	2.28 (0)	7.0 (7.9) [2]	58.6 (65.7)
LNH-Lactate(p)[b]	7.81 (7.81)	2.33 (2.98)	0 (0)	13.1 (12.3) [2]	38.1 (37.2)
LNH-Lactate(ae)	12.58 (13.08)	3.06 (3.67)	2.55 (0)	7.7 (6.5) [1]	40.3 (49.1)
LNH-NO$_3$(p)[c]	1.82 (0)	1.83 (2.11)	1.69 (2.82)	6.8 (7.3) [1]	31.6 (29.6)
LNH-NO$_3$(ae)	8.45 (0)	2.22 (2.83)	5.06 (5.64)	7.9 (7.3) [1]	41.2 (39.9)

[a] The content of water was determined using DTA/DTG analysis, m is the number of water molecules. [b] Assuming 40 % β-Ni(OH)$_2$. [c] Assuming 50 % β-Ni(OH)$_2$.
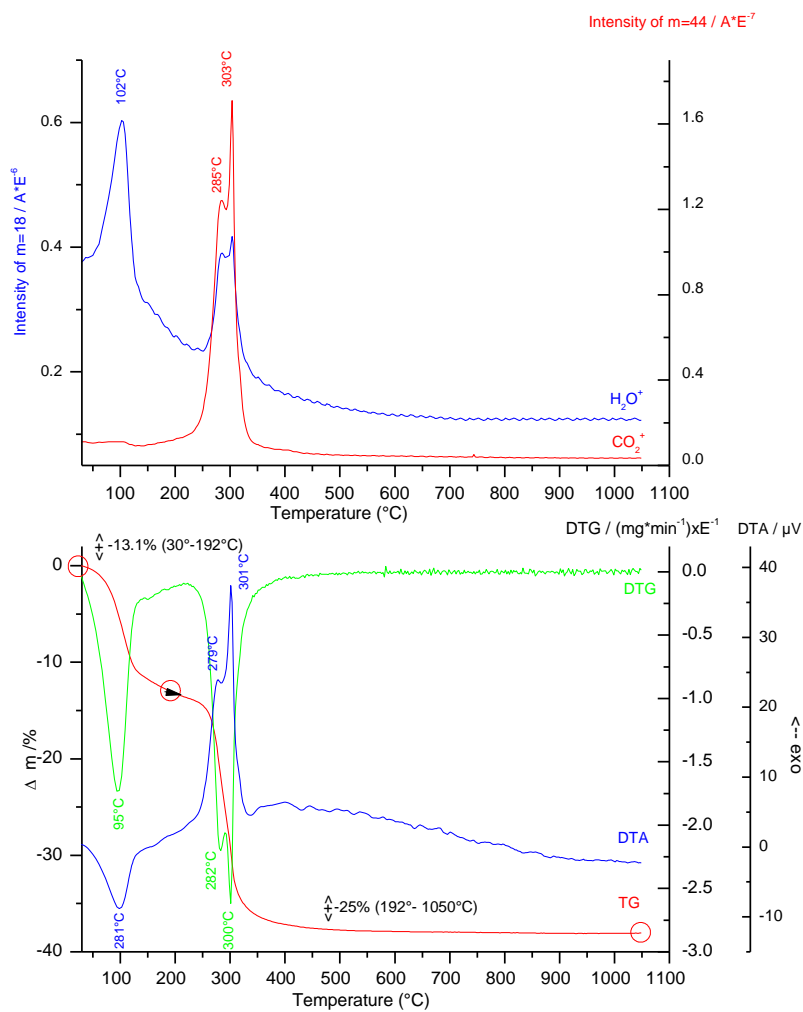
Figure S1. TGA/DTA/MS curves and the evolution of gases for LNH-Lactate(p). The measurements were performed in a synthetic air atmosphere (flow rate 30 mL min^{-1}) from 30 to 1050 °C with a heating rate of 5 °C min^{-1}.
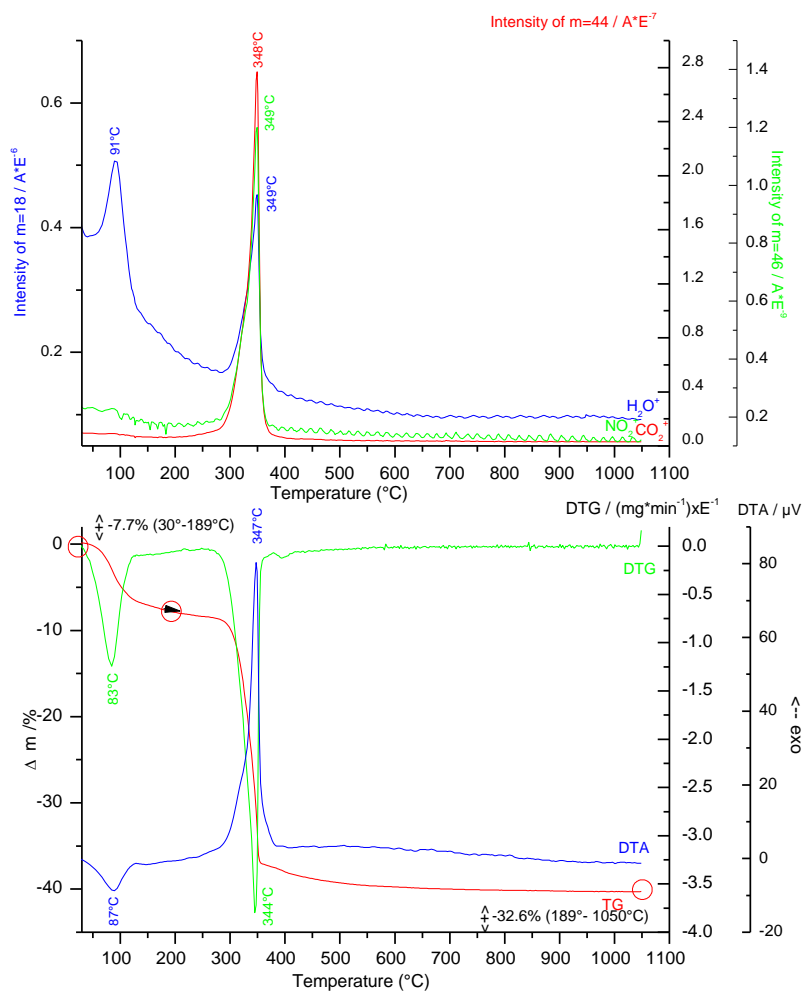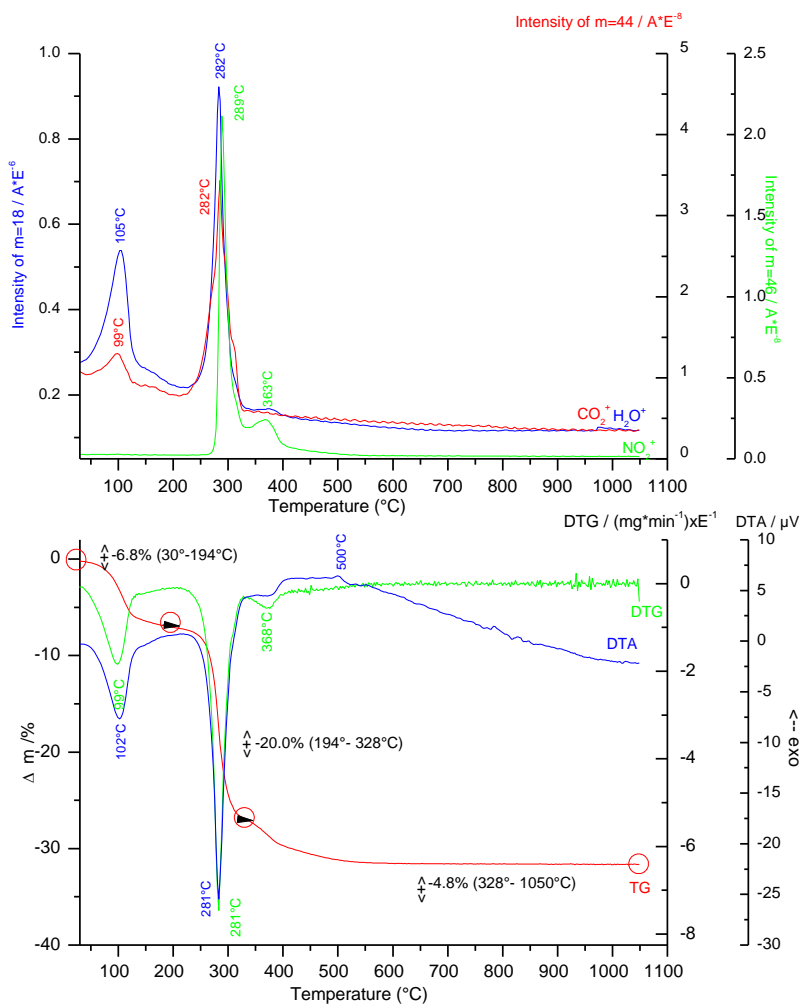
Figure S2. TGA/DTA/MS curves and the evolution of gases for LNH-Lactate(ae). The measurements were performed in a synthetic air atmosphere (flow rate 30 mL min^{-1}) from 30 to 1050 °C with a heating rate of 5 °C min^{-1}.

Figure S3. TGA/DTA/MS curves and the evolution of gases for LNH-NO$_3$(p).
The measurements were performed in a synthetic air atmosphere (flow rate 30 mL min^{-1})
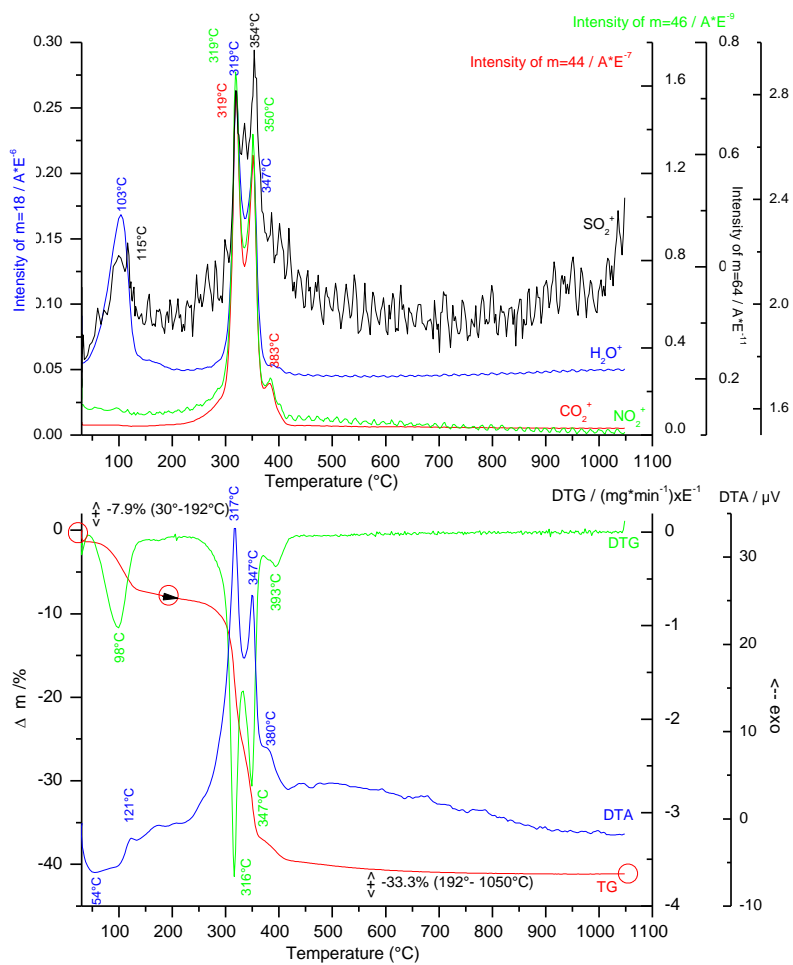from 30 to 1050 °C with a heating rate of 5 °C min^{-1}.

Figure S4. TGA/DTA/MS curves and the evolution of gases for LNH-NO$_3$(ae). The measurements were performed in a synthetic air atmosphere (flow rate 30 mL min^{-1}) from 30 to 1050 °C with a heating rate of 5 °C min^{-1}.

Figure S5. Powder XRD patterns of LNH-DS measured in the transmission mode. The diffraction peak of the Mylar foil support is labelled (●).
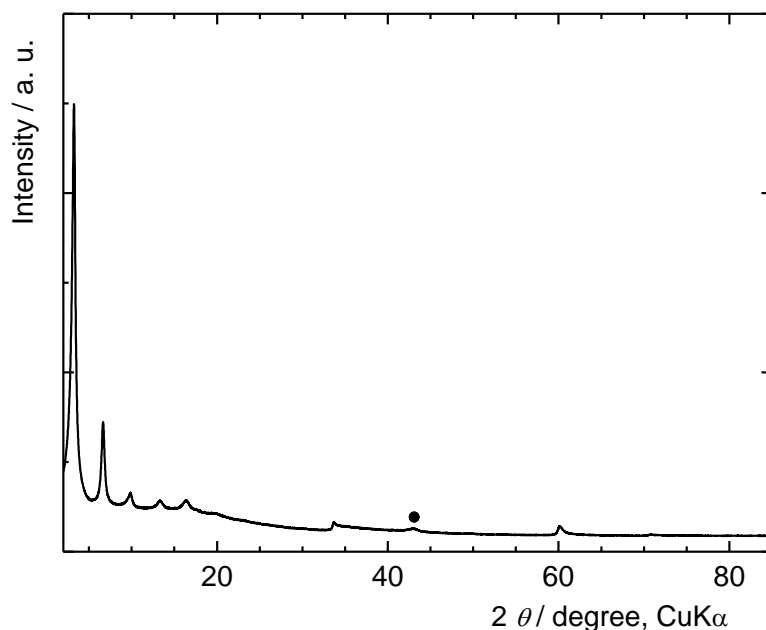

Figure S6. FTIR spectrum of LNH-DS: (a) Broad band between 3750 - 3100 cm^{-1} is due to the stretching vibrations of hydroxyl groups. (b) Sharp bands at 2956, 2924, and 2854 cm^{-1} arise from the C-H stretching vibrations of the dodecyl chain. (c) Peak at 1635 cm^{-1} corresponds to the $\delta(H_2O)$ vibrations. (d) Peak at 1468 cm^{-1} is caused by the bending vibrations of the CH_2 groups. (f, g) 1193 and 1055 cm^{-1} peaks arise from the stretching vibrations of the SO_3 groups. These peaks together with the peak at 980 cm^{-1} (h) obscure three peaks of HMT, which is present as an impurity. (e) Peak at 1340 cm^{-1} belongs to HMT.
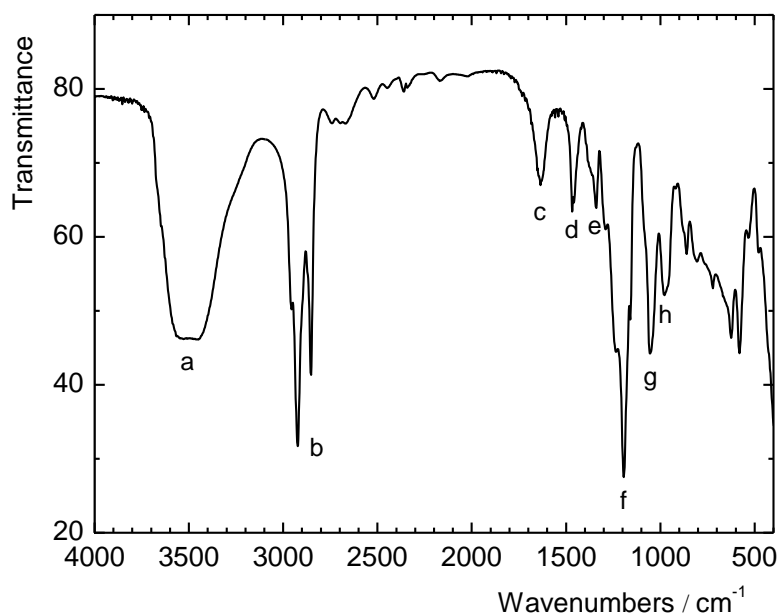
Figure S7. UV-Vis absorption spectra of the LNH-Lactate(ae) dispersion (a, red curve) and the self-standing film (b, black curve).
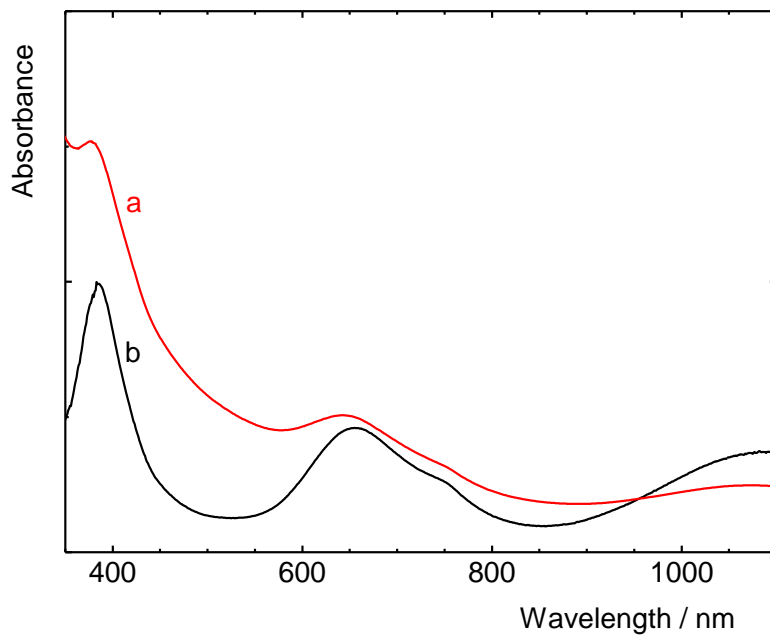

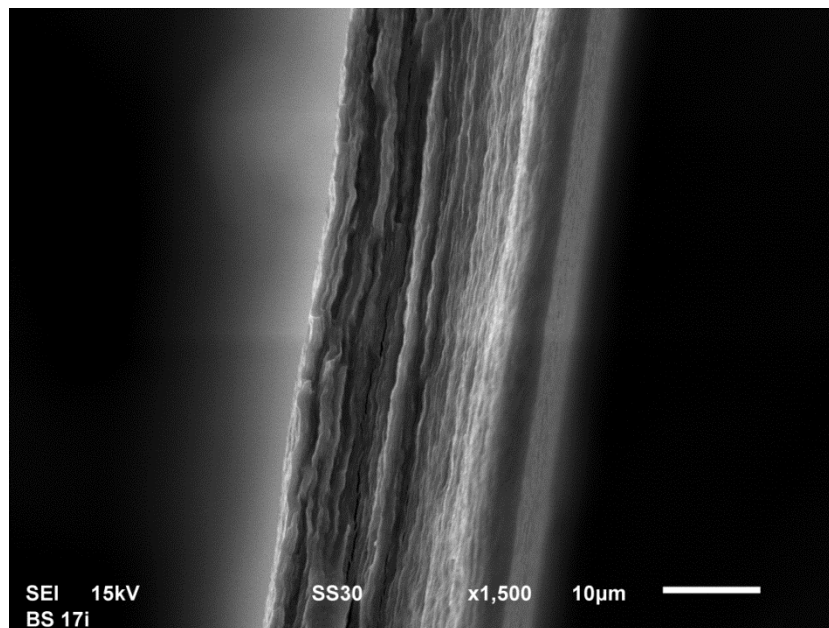**Figure S8.** SEM image of the LNH-Lactate(ae) self-standing film.

Figure S9. XRD patterns of the film prepared from delaminated LNH-Lactate(p) measured in the reflection (a) and transmission (b) modes. The diffractions of LNH-Lactate(p) (♦), β-$Ni(OH)_2$ (▲), and the Mylar foil support (●) are labelled. The diffractograms are vertically shifted to avoid overlaps.
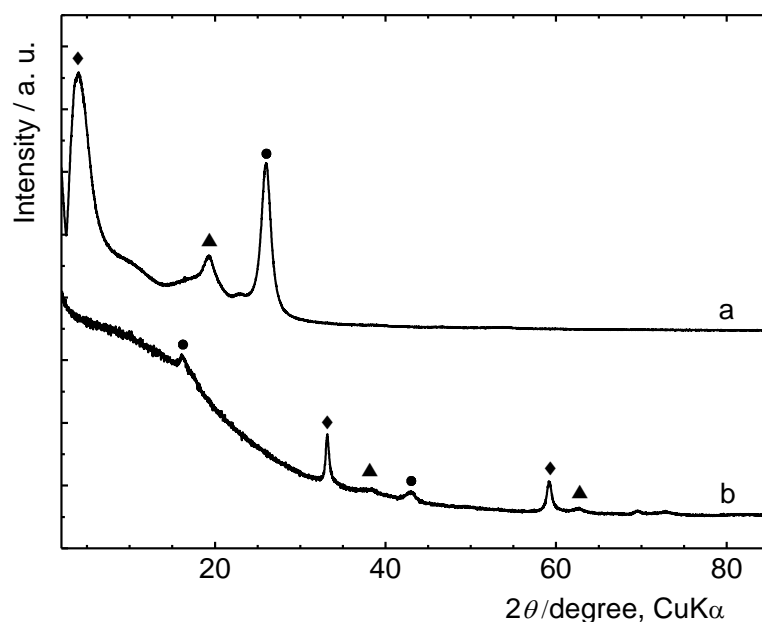

Figure S10. XRD patterns of the film prepared from delaminated LNH-NO_3(p) measured in the reflection (a) and transmission (b) modes. The diffractions of LNH-NO_3(p) (♦),β-$Ni(OH)_2$ (▲), and the Mylar foil support (●) are labelled. The diffractograms are vertically shifted to avoid overlaps.
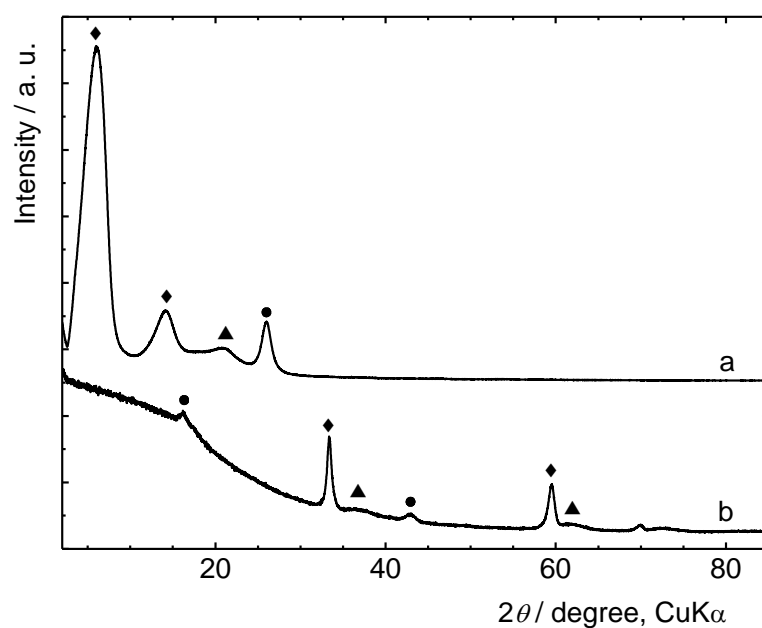
Figure S11. XRD patterns of the LNH-Lactate(ae) self-standing film in the reflection (a) and transmission (b) modes. The diffractions of LNH-Lactate(ae) (♦) and the Mylar foil support (●) are labelled. The diffractograms are vertically shifted to avoid overlaps.
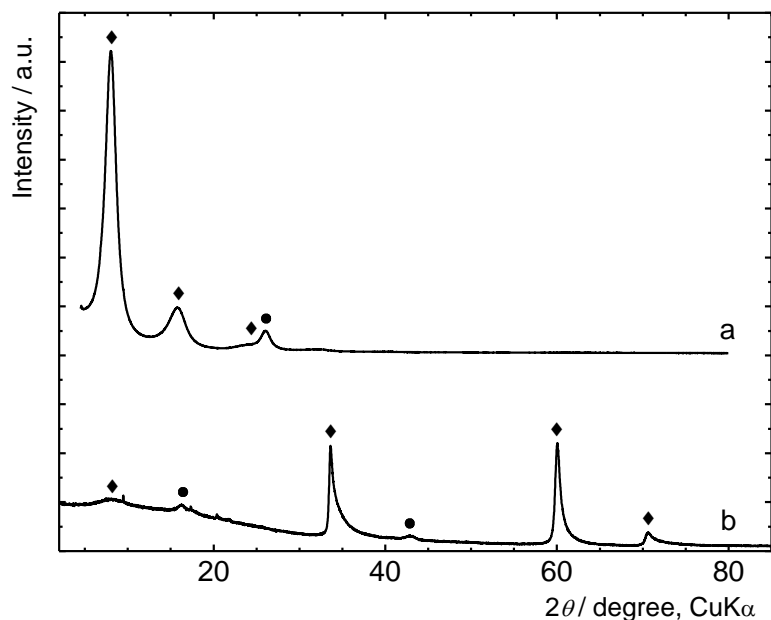

Figure S12. SAXS curves of LNH-Lactate(ae) aqueous dispersions at various concentrations: (a) 1 g L^{-1}; (b) 2 g L^{-1}; (c) 4 g L^{-1}. The tails of the curves for $q > 0.5$ Å^{-1} obtained for various concentrations coincided, which suggest that the scattering contribution of the particles in this region can be neglected and that the measured intensity can be ascribed to scattering from the solvent.
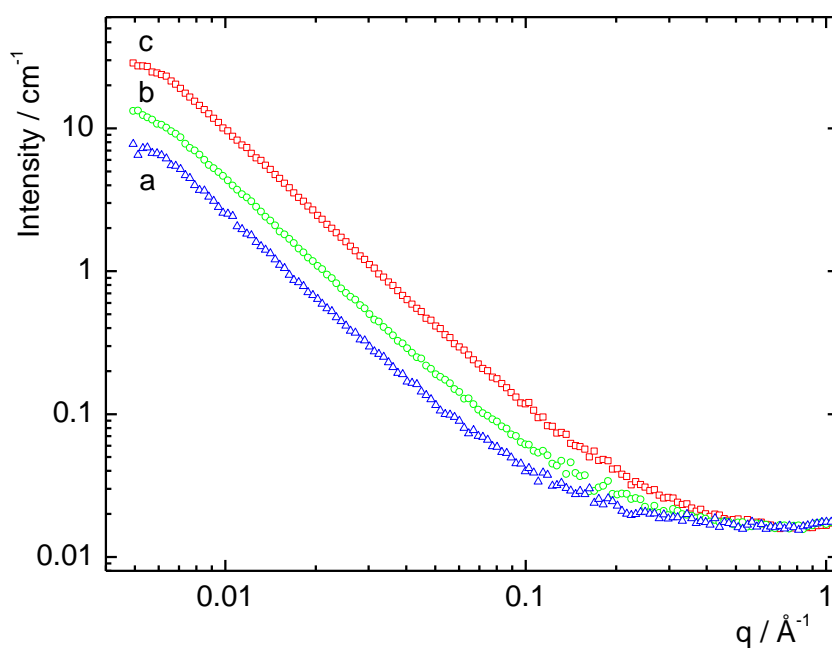
Figure S13. AFM image of LNH-Lactate(p) nanolamellar units (blue circle) and their prevailingly 2D-aggregates (red circle) deposited by spin coating on a mica substrate.
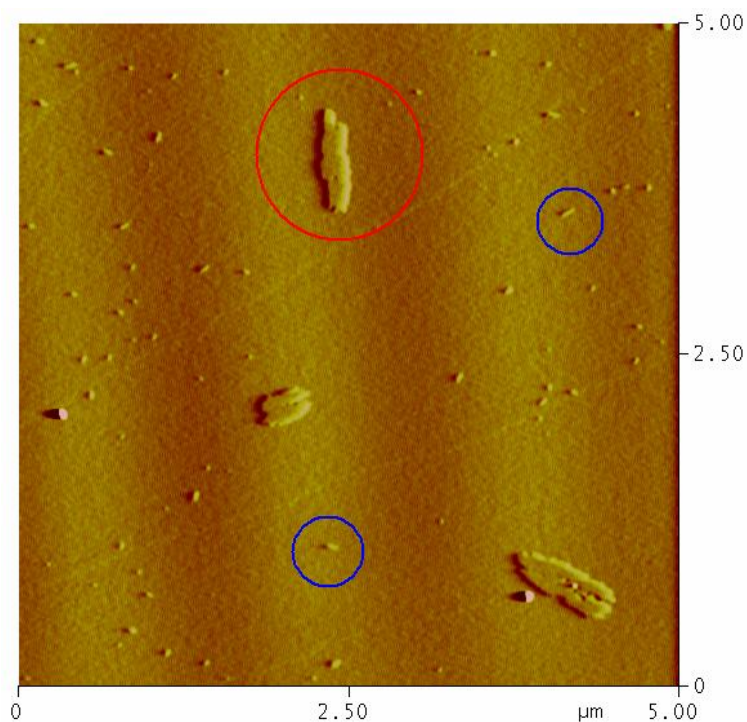

Figure S14. Profile analysis of the lateral size of LNH-Lactate(p) lamellar aggregates spin coated on a mica support. The height profiles revealed that both the nanolamellar units (left) and their aggregates (right) have almost identical thickness (~ 1 nm).
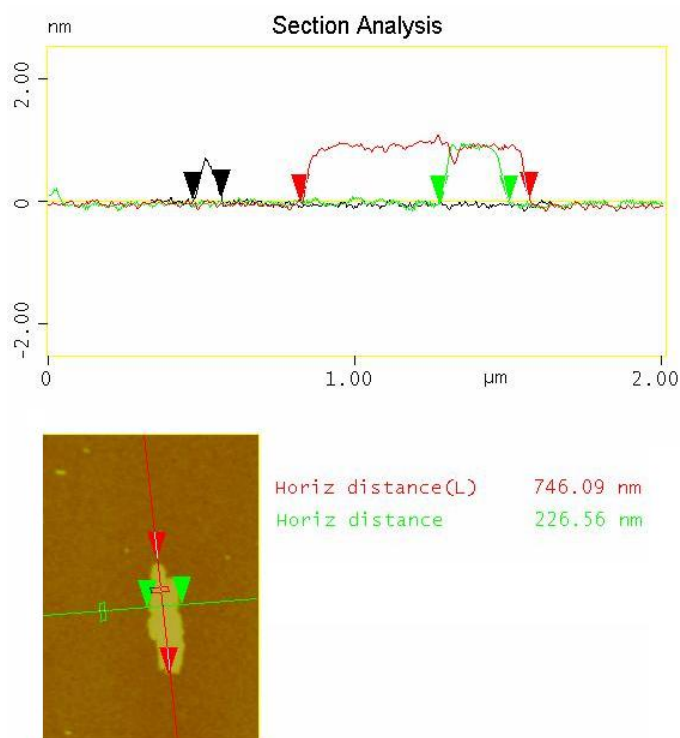
Figure S15. Maximum height (Zmax) distribution curve (right, black dots) of the area covered by the LNH-Lactate(p) single units shows a maximum close to 1 nm. The best fit curve is shown in red (Gaussian). The plotted height data were acquired from AFM-imaged topography (left).
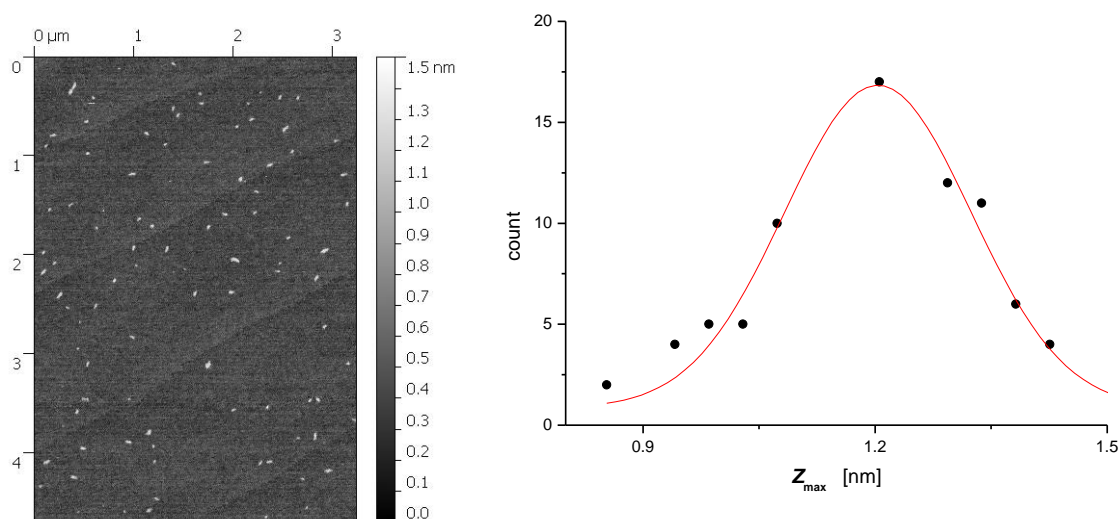

Figure S16. Height (Z) density distribution (σ) curve (right) measured on a LNH-Lactate(ae) deposit indicates a preferable single-layer (2D) growth, (Z maximum is close to 1 nm). A maximum Z approximately at 2.5-2.8 nm can be assigned to more stacked hydroxide layers (it is approximately a 10% fraction of the aggregate). The plotted height data (right) were acquired from AFM-imaged topography (left).
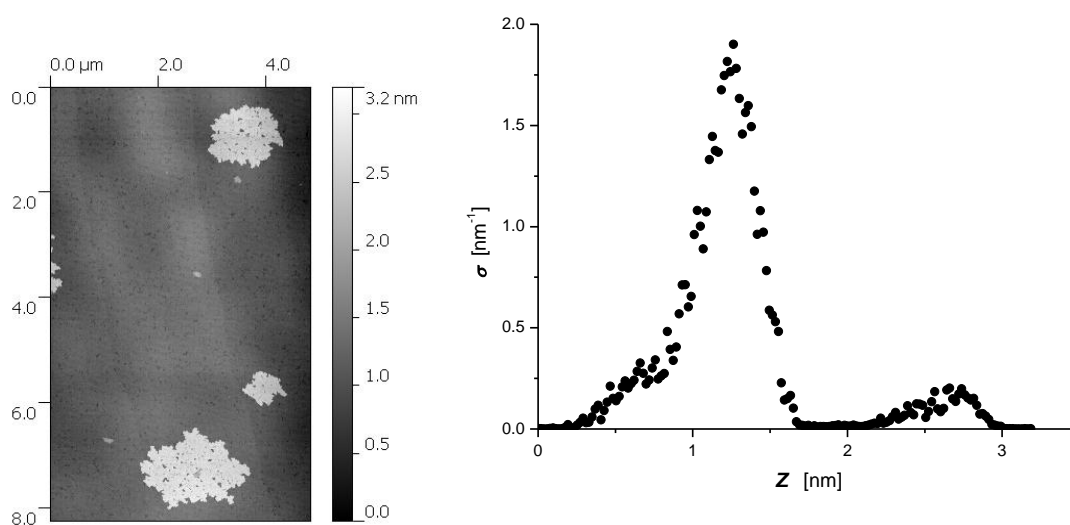

S14

Figure S17. Profile analysis of aggregates of the LNH-NO$_3$(p) nanosheets prepared by spin coating on a mica support. The analysis shows an aggregate height of 1.3 nm.
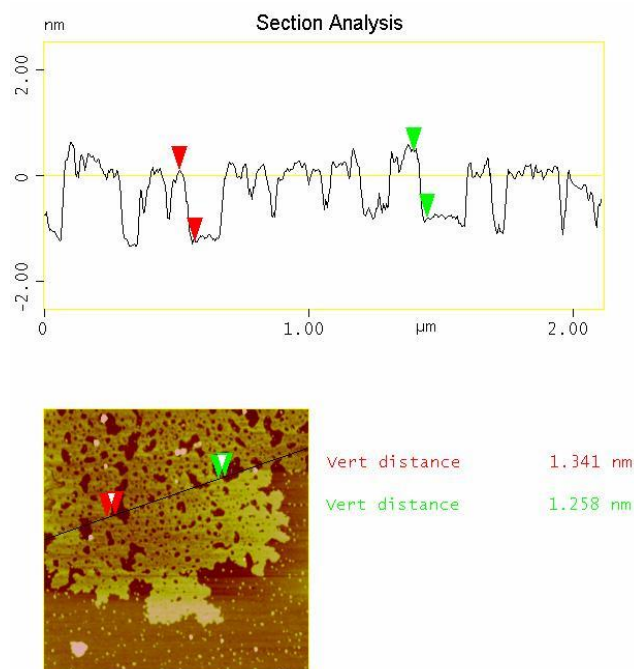

Figure S18. High-resolution TEM image at the centre of a LNH-Lactate(ae) nanosheet and the computed FFT pattern ($d_1 = 4.1 \pm 0.5$ Å, $d_2 = 2.3 \pm 0.5$ Å, $d_3 = 2.0 \pm 0.5$ Å).
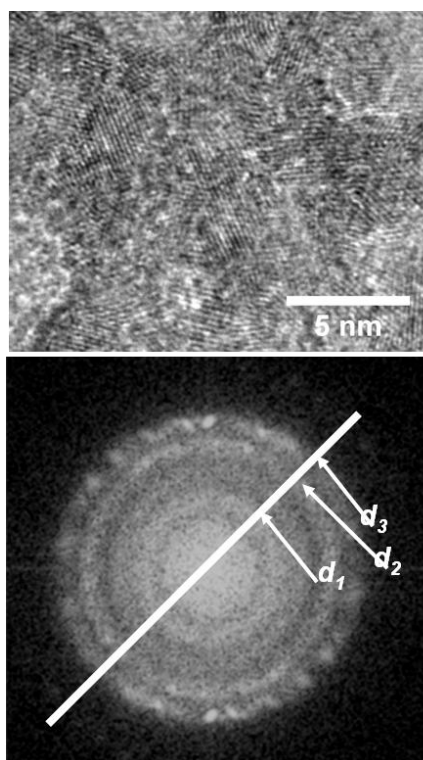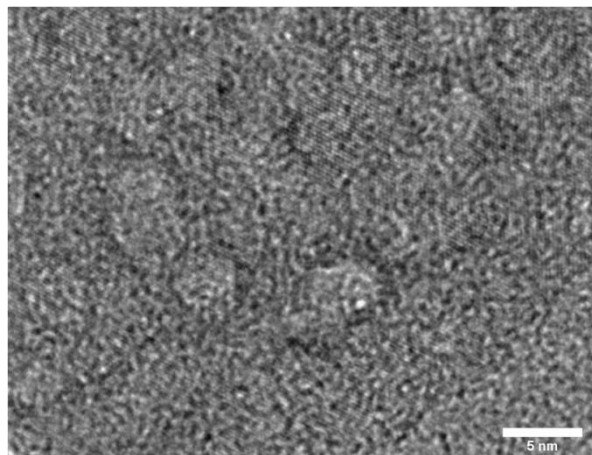
Figure S19. A) High-resolution TEM image of the LNH-NO$_3$(p) nanosheets showing the discontinues atomic planes within a platelet. B) SAED pattern (d_1 = 2.50 ± 0.05 Å, d_2 = 1.50 ± 0.05 Å, d_3 = 1.45 ± 0.05 Å, d_4 = 1.27 ± 0.05 Å).

A)

B)